Rapid and Permanent Neuronal Inactivation In Vivo via Subcellular Generation of Reactive Oxygen with the Use of KillerRed

Cell Reports
Resource

Rapid and Permanent Neuronal Inactivation In Vivo via Subcellular Generation of Reactive Oxygen with the Use of KillerRed

Daniel C. Williams,[1,5,6] Rachid El Bejjani,[1,5] Paula Mugno Ramirez,[2,5] Sean Coakley,[2,5] Shin Ae Kim,[3] Hyewon Lee,[3] Quan Wen,[4] Aravi Samuel,[4] Hang Lu,[3,*] Massimo A. Hilliard,[2,*] and Marc Hammarlund[1,*]
[1]Department of Genetics and Program in Cellular Neuroscience, Neurodegeneration and Repair, Yale University, New Haven, CT 06510, USA
[2]Queensland Brain Institute, The University of Queensland, Brisbane, QLD 4072, Australia
[3]School of Chemical & Biomolecular Engineering, Georgia Institute of Technology, Atlanta, GA 30332, USA
[4]Department of Physics and Center for Brain Science, Harvard University, Cambridge, MA 02138, USA
[5]These authors contributed equally to this work
[6]Present address: Department of Biology, Coastal Carolina University, Conway, SC 29526, USA
*Correspondence: hang.lu@gatech.edu (H.L.), m.hilliard@uq.edu.au (M.A.H.), marc.hammarlund@yale.edu (M.H.)
http://dx.doi.org/10.1016/j.celrep.2013.09.023

SUMMARY

Inactivation of selected neurons in vivo can define their contribution to specific developmental outcomes, circuit functions, and behaviors. Here, we show that the optogenetic tool KillerRed selectively, rapidly, and permanently inactivates different classes of neurons in *C. elegans* in response to a single light stimulus, through the generation of reactive oxygen species (ROS). Ablation scales from individual neurons in single animals to multiple neurons in populations and can be applied to freely behaving animals. Using spatially restricted illumination, we demonstrate that localized KillerRed activation in either the cell body or the axon triggers neuronal degeneration and death of the targeted cell. Finally, targeting KillerRed to mitochondria results in organelle fragmentation without killing the cell, in contrast to the cell death observed when KillerRed is targeted to the plasma membrane. We expect this genetic tool to have wide-ranging applications in studies of circuit function and subcellular responses to ROS.

INTRODUCTION

Optogenetic approaches to studying the function of specific neurons in vivo generally involve the use of light to acutely activate or inactivate the cells of interest. In particular, inactivation in *Caenorhabditis elegans* of specific neurons in vivo can be used to investigate their contribution to specific network functions and also to study compensation or homeostasis in the remaining cells. However, the best-described optogenetic tools for silencing neurons in *C. elegans*, halorhodopsin (Zhang et al., 2007) and archaerhodopsin (Chow et al., 2010; Okazaki et al., 2012), are light-driven ion pumps (chloride and protons, respectively) that require constant stimulation to keep neurons inactive, and may not be suitable for studying behavior, compensation, or homeostasis over longer timescales.

An alternative way to acutely and permanently inactivate specific neurons in vivo is to kill them. Investigators have utilized this approach extensively in *C. elegans* to define the function of a wide variety of cells (especially neurons), using a laser microbeam to ablate the cells (Avery and Horvitz, 1987, 1989; Fang-Yen et al., 2012). However, application of the laser-ablation approach is limited because of the difficulty of ablating multiple target cells without damaging surrounding cells or tissues, and the extensive amount of time required to perform surgery on a large number of animals. Thus, the development of optogenetic ablation tools that can be spatially and temporally controlled is highly desirable. An optimal optogenetic ablation tool should kill cells rapidly, avoid collateral damage to neighboring cells and tissues, and scale in application from single neurons to groups of cells in single animals or populations.

KillerRed is a dimeric red fluorescent protein that produces high levels of reactive oxygen species (ROS) upon illumination with green light (540–580 nm), thereby inducing cell death (Bulina et al., 2006). Structurally, KillerRed resembles other GFP-like proteins, which comprise an 11-strand antiparallel β-barrel that surrounds a centrally located chromophore (Carpentier et al., 2009; Pletnev et al., 2009). However, KillerRed is 1,000 times more toxic than other fluorescent proteins. This higher toxicity is due to the presence of a long water-filled channel in KillerRed that allows diffusion of molecular oxygen near the chromophore, and is thought to provide a path for electron transfer during the production of superoxide radicals (Roy et al., 2010; Serebrovskaya et al., 2009). Similar to the generation of GFP fluorescence, the phototoxic activity of KillerRed is effective in vivo and can be induced in mammalian and zebrafish cells without coexpression of other factors (Bulina et al., 2006; Teh et al., 2010).

Cell PRESS
Open ACCESS

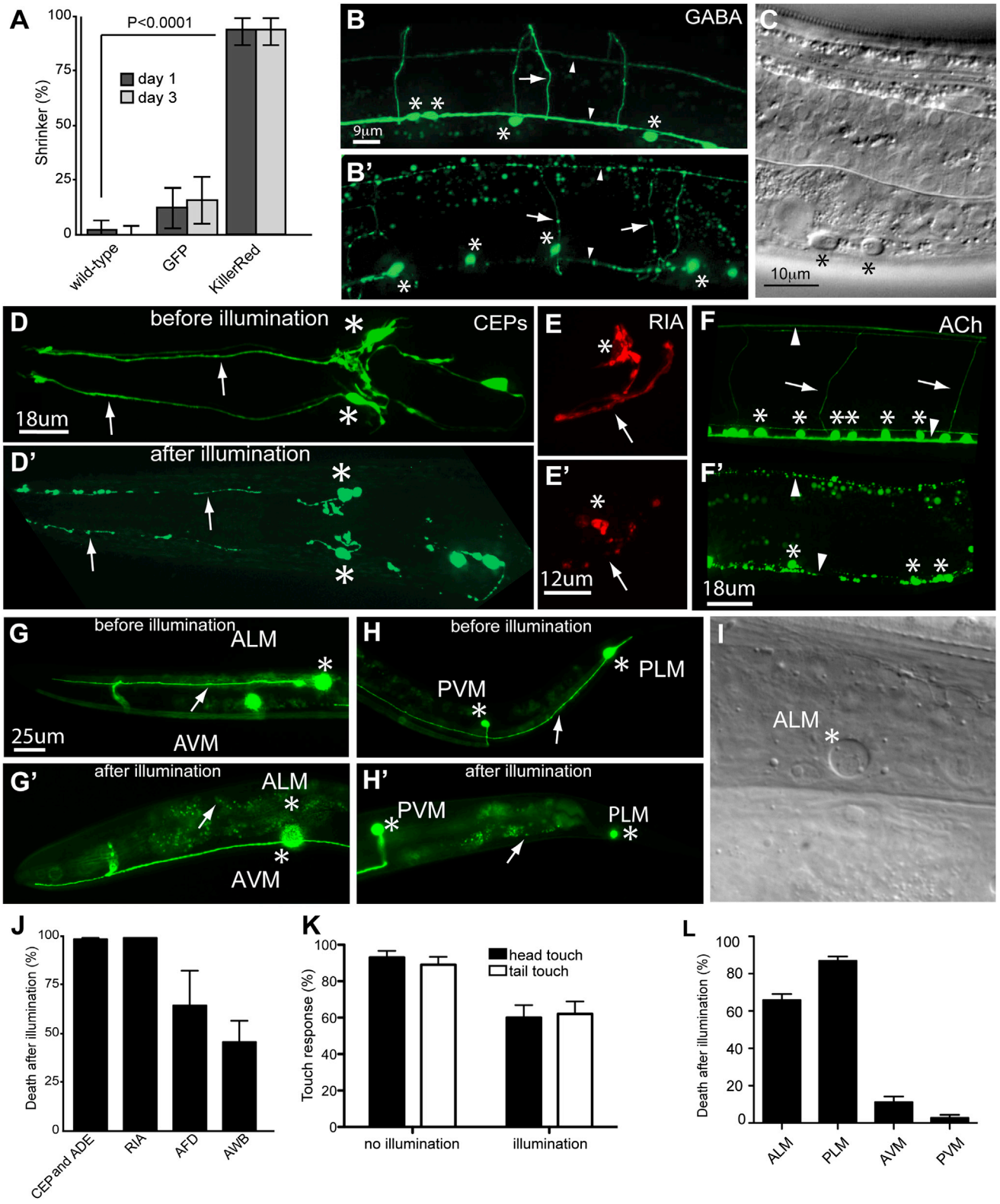

Figure 1. KillerRed Activation Disrupts the Function and Morphology of Targeted Neurons and Results in Cell Death

(A) KillerRed activation induces behavioral defects. Animals were illuminated with white light and then scored 24 and 72 hr later for the shrinker phenotype caused by GABAergic neuron dysfunction. n = 50 for KillerRed and GFP, and 100 for wild-type.

(legend continued on next page)

Here, we demonstrate that KillerRed can efficiently kill a variety of neurons in *C. elegans*, including sensory neurons, interneurons, and motor neurons. We show that the effect of KillerRed is cell-autonomous and does not spread to nearby neurons. Our results indicate that KillerRed disruption of neuronal function is rapid and can be used to alter the circuits and behavior of freely moving animals. In addition, the tool is highly modifiable, with ablation efficiency dependent upon illumination duration and intensity. We also demonstrate that certain neurons are resistant to KillerRed damage, raising the intriguing possibility that some cells possess increased intrinsic protection mechanisms against ROS. We further show that subcellular localization of KillerRed dramatically alters its function, with mitochondria localization resulting in specific disruption of organelle morphology. Finally, using selective illumination, we show that exposure of individual neuronal compartments, such as the cell body or the axon, is sufficient to induce neuronal damage and death.

RESULTS

Expressing KillerRed in *C. elegans* GABA Neurons Results in Light-Dependent Cell Death

We established the consequences of KillerRed activation in different sets of *C. elegans* neurons, including motor neurons, mechanosensory neurons, chemosensory neurons, and interneurons (details of the KillerRed constructs and illumination parameters can be found in Table S1 available online). We first generated transgenic animals expressing cytosolic KillerRed under the control of the GABAergic neuron-specific promoter *Punc-47*, which drives expression in 26 motor neurons required for coordinated movement (McIntire et al., 1997). Cytosolic KillerRed activation in GABAergic neurons caused a "shrinker" phenotype (i.e., longitudinal shortening of the body upon head touch) in the animals 24 hr after illumination, consistent with loss of GABAergic neuronal function (Figure 1A; McIntire et al., 1993). Furthermore, neuronal function remained disrupted 72 hr after KillerRed activation (Figure 1A), suggesting that the affected neurons were dead rather than merely damaged. To examine the morphology of KillerRed-expressing neurons before and after KillerRed activation, we coexpressed GFP in the targeted cells (Figure 1B). Twenty-four hours after KillerRed activation, we found that the morphology of the GABAergic neurons was severely disrupted, with axonal processes that were fragmented and broken, often with large blebs, or missing altogether (Figure 1B′). The cell bodies of the affected neurons were round and swollen, and appeared smaller than those in nonilluminated animals, consistent with neuronal death. To confirm that the morphological changes observed based on GFP fluorescence reflected cell death, we analyzed the GABAergic neurons by differential interference contrast (DIC) microscopy and found that the cell bodies of affected neurons displayed swelling, the presence of vacuole-like structures, and nuclear changes (Figure 1C), all of which are phenotypes consistent with cell death.

The observed structural and behavioral defects were specific and dependent on KillerRed expression and activation. Illumination of either wild-type animals or animals expressing only GFP in GABAergic neurons did not elicit a shrinker phenotype (Figure 1A). Moreover, expression and illumination of the spectrally similar fluorophore mCherry did not cause a detectable behavioral defect (data not shown). Furthermore, prior to illumination, neurons expressing KillerRed displayed no morphological or functional deficits, indicating that neuronal death was dependent upon KillerRed activation (Figures 1A and 1B). Thus, KillerRed activation in GABAergic neurons permanently disrupts function and results in cell death.

KillerRed Can Be Used to Efficiently Ablate Multiple Classes of Neurons

Our experiments demonstrated that KillerRed can disrupt neuronal function. Next, we asked whether we could improve the efficiency of disruption. KillerRed is dimeric (Bulina et al., 2006; Carpentier et al., 2009; Pletnev et al., 2009), and we reasoned that increased efficiency might result from expression as a tandem dimer, as previously reported for other multimeric fluorescent proteins (Campbell et al., 2002; Shaner et al., 2004). We generated a tandem-dimer version of KillerRed (tdKillerRed) and found that it was significantly more effective than monomeric KillerRed at disrupting GABA neuron function. After illumination with green light (5.1 mW/mm^2 for 5 min), 100% of tdKillerRed animals (n = 11) exhibited a shrinker phenotype, compared with only 14% for monomeric KillerRed (n = 14; $p < 0.0001$). We also localized tdKillerRed to the plasma membrane using a myristoylation tag (myr-tdKillerRed). Membrane-targeted dimeric KillerRed had efficiency similar to that of soluble dimeric KillerRed (92% shrinker, n = 13, p = 1.0). We

(B and B′) Confocal images of the GABAergic nervous system of GABA::KillerRed (*Punc-47::KillerRed*) animals before (B) and 24 hr after (B′) illumination.
(C) Nomarski image of affected GABAergic neuron cell bodies 24 hr after KillerRed activation.
(D and D′) CEPs before (D) and 24 hr after (D′) illumination. After illumination, the dendrites of CEP neurons (arrows) are fragmented and the cell bodies (asterisks) are smaller and rounded.
(E and E′) RIA interneuron before (E) and 24 hr after (E′) illumination, with the cell body and axon degenerated in (E').
(F and F′) Cholinergic nervous system before (F) and 24 hr after (F′) illumination. Activation results in fragmentation of neuronal processes as well as fewer and smaller cell bodies.
(G–H') Fluorescent images of axonal and neuronal damage in ALM and PLM before (G and H) and 24 hr after (G' and H') illumination. After illumination, ALM is completely cleared (G′) and the PLM axon has disappeared (H').
(I) Nomarski image of ablated ALM cell body 24 hr after illumination.
(J) Quantification of cell death 24 hr after illumination. n = 155 cells (CEP and ADE), 48 cells (RIA), 74 cells (AWB), and 17 cells (AFD).
(K) Light touch response 24 hr after illumination in wild-type and KillerRed-expressing animals. After KillerRed activation, there is a reduction in the response to light touch in both the head and tail of the animal. n = 50 animals.
(L) Quantification of cell death in touch neurons 24 hr after illumination. n = 107 cells (AVM and PVM) and 214 cells (ALM and PLM). In all figures, asterisks mark neuron cell bodies, arrows mark processes, and arrowheads mark dorsal and ventral nerve cords. Error bars indicate 95% confidence intervals.
See also Table S1.

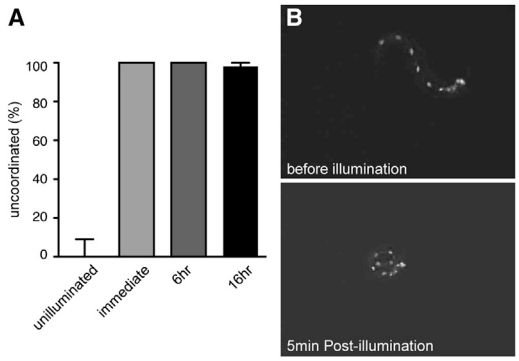

Figure 2. KillerRed Activation Results in Immediate Disruption of Neuronal Function

(A) Illumination of animals expressing KillerRed in cholinergic neurons results in immediate and permanent disruption of movement. n = 50 for unilluminated, n = 20 for immediate (just after the end of illumination) and 6 hr time points, and n = 41 for 16 hr time point. Error bars indicate 95% confidence intervals.

(B) A freely swimming L1 larva before KillerRed activation in GABAergic motor neurons (top panel). The same larva immediately following 5 min exposure to green light illumination (~40 mW/mm^2) displays uncoordinated locomotion (bottom panel).

See also Table S1.

used myr-tdKillerRed for some of the subsequent experiments (Table S1).

To determine whether other neurons could be targeted by KillerRed, we generated different transgenic strains expressing KillerRed in the dopaminergic neurons CEP, ADE, and PDE (*Pdat-1::myr-tdKillerRed*); the interneuron RIA (*Pglr-3::myr-tdKillerRed*); the cholinergic neurons (approximately 120 neurons; *Punc-17::myr-tdKillerRed*); the amphid sensory neurons AWB (*Pstr-1::myr-tdKillerRed*) and AFD (*Pgcy-8::myr-tdKillerRed*); and the mechanosensory neurons ALM (L/R), PLM(L/R), AVM, and PVM (*Pmec-4::KillerRed*). Like the GABAergic motor neurons, the dopaminergic neurons CEP and ADE and the interneuron RIA were efficiently killed after KillerRed activation (Figures 1D, 1E, and 1J). The cholinergic neurons were also efficiently killed, although the maximum efficiency could not be determined because the animals died (Figure 1F). This lethal phenotype is consistent with a requirement for cholinergic neuron function for survival of animals in early developmental stages (Alfonso et al., 1993). In comparison with these cell types, the AWB and AFD amphid neurons were killed with lower efficiency (Figure 1J). The dopaminergic PDE neurons were also killed with lower efficiency (26 out of 60 cells), even though the other dopaminergic neurons were efficiently killed in the same animals. We also tested the efficiency of KillerRed in the mechanosensory neurons, which mediate a specific behavior: response to light touch. We found that expression and activation of KillerRed in the mechanosensory neurons caused deficits in mechanosensation (Figure 1K). Consistent with this loss of touch sensitivity, KillerRed activation also caused efficient neuronal cell death in ALM and PLM neurons (Figures 1G–1I and 1L). However, the AVM and PVM neurons were refractory to axonal degeneration or cell death. Thus, KillerRed can ablate many neuronal types in *C. elegans*, and is effective at targeting single neurons as well as entire neuronal classes, with selected neurons being specifically resistant to disruption.

KillerRed Induces Immediate Inactivation of Illuminated Neurons

Although the morphological effects of KillerRed activation in neuronal cell bodies and processes are not apparent immediately after activation, it is possible that KillerRed disrupts neuronal function more rapidly than it affects neuronal morphology. To test this, we used two strategies. First, we took advantage of the profound consequence of KillerRed activation in cholinergic neurons, which triggers paralysis in a coiled posture, similar to what is observed in animals that lack cholinergic neurotransmission (Rand, 1989). To determine the time necessary for neuronal function to be disrupted by KillerRed activation, we quantified this uncoordinated behavior at various times after illumination. This revealed that functional disruption was both immediate and permanent (Figure 2A). Immediately after completion of the 5 min illumination period, the animals exhibited a robust, uncoordinated phenotype consistent with loss of cholinergic neuron function. This functional deficit persisted long after activation, suggesting that disruption was not due to temporary inactivation, but rather to permanent disruption of neuronal function followed by cell death.

Second, we used an optogenetic illumination system that allowed us to expose single, freely swimming animals to intense green laser light while monitoring their behavior before, during, and after illumination (Leifer et al., 2011). When we used this system to analyze the effect of KillerRed activation in GABAergic motor neurons of freely swimming L1 larvae, we found that activation of KillerRed caused a severe deficit in locomotion, which was observed immediately after the end of the illumination period (Figure 2B; Movies S1 and S2). Together, these experiments demonstrate that KillerRed activation can rapidly and permanently disrupt neuronal function. In addition, our inactivation experiments in the GABAergic neurons of L1 animals suggest that these neurons make a greater contribution to normal locomotion of L1 animals than was previously appreciated.

KillerRed-Dependent Neuronal Death Is Caspase Independent and Can Be Improved by Mutating ROS-Detoxifying Enzymes

KillerRed is thought to act as a type II photosensitizer, producing superoxide anion radicals rather than singlet oxygen (Pletnev et al., 2009; Shu et al., 2011). Superoxide is scavenged by superoxide dismutases (SODs), which catalyze the conversion of superoxide radicals to hydrogen peroxide and thus limit cellular damage. *C. elegans* has a total of five SODs, two of which (*sod-1* and *sod-5*) are cytoplasmic Cu/Zn SODs (the remaining three SODs are mitochondrial Fe/Mn SODs [*sod-2* and *sod-3*] and an extracellular Cu/Zn SOD [*sod-4*]) (Landis and Tower, 2005). We found that a *sod-1* mutant background, which eliminates one of the cytoplasmic SODs, increased the efficiency of ablation in AWB, a neuron that normally is refractory to KillerRed damage (Figure 3A). These data support a model in which KillerRed exerts its effect via superoxide, and demonstrate that the effect of KillerRed in normally resistant cells can be enhanced by specific genetic mutations.

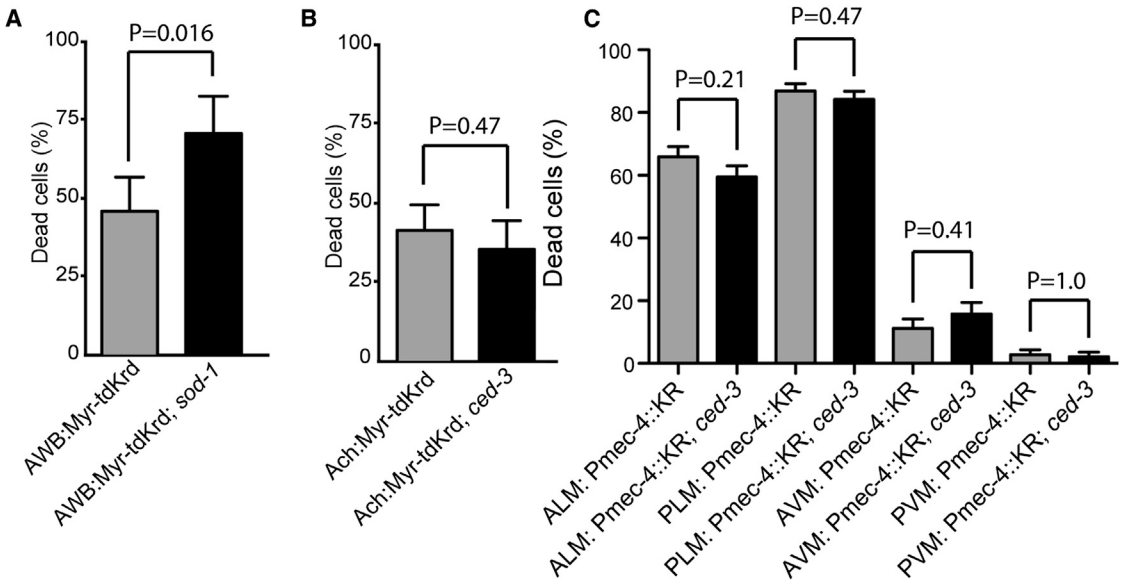

Figure 3. KillerRed Phototoxicity Is Enhanced in SOD Mutants and Does Not Require the Caspase CED-3

(A) Myr-tdKillerRed activation ablates AWB amphid neurons more effectively in *sod-1(tm776)* mutant animals. n = 74 cells (wild-type) and 38 cells (*sod-1*).

(B) Neuronal cell death induced by Myr-tdKillerRed activation in cholinergic neurons does not require *ced-3(n717)*. The illumination protocol was adjusted to avoid killing the animals (see Table S1). n = 132 cells (wild-type) and 79 cells (*ced-3*).

(C) Neuronal cell death induced by cytosolic KillerRed activation in mechanosensory neurons does not require *ced-3(n717)*. For *ced-3*, n = 95 cells (AVM, PVM) and 190 cells (ALM, PLM); for wild-type, n = 107 cells (AVM and PVM) and 214 cells (ALM and PLM; same data as Figure 1L). Phenotypes were determined 24 hr after illumination. In all panels, error bars indicate 95% confidence intervals.

See also Table S1 and Movies S1 and S2.

In *C. elegans*, apoptotic cell death requires the caspase CED-3, whereas necrotic cell death does not (Ellis and Horvitz, 1986; Hall et al., 1997). We tested whether KillerRed-mediated neuronal cell death occurred through apoptosis by examining the requirement for *ced-3*. Cell death, as well as the other morphological and behavioral consequences of KillerRed activation, was as robust in *ced-3* mutants as in the wild-type for both acetylcholine motor neurons and mechanosensory neurons (Figures 3B and 3C). Further, the pathology of neuronal cell death induced by KillerRed included cell swelling, vacuolation, and nuclear changes (Figures 1C and 1I), which is similar to previous observations of necrosis-like neuronal cell death (Hall et al., 1997) but in contrast to the compact morphology of apoptotic cells. These observations suggest that KillerRed does not act via an apoptotic pathway and may instead kill neurons through a necrotic, caspase-independent mechanism.

KillerRed's Effects Are Cell Autonomous and Do Not Spread to Adjacent Neurons

To test the cell autonomy of KillerRed's cytotoxicity, we examined the morphology of neurons located adjacent to KillerRed-targeted cells in three different experiments. First, we examined AWA and AWB, which are sensory neurons located in the head. The cell bodies of the AWA and AWB neurons are located next to each other within the lateral ganglia; their axons project into the nerve ring and their dendrites fasciculate with each other (White et al., 1986). We found that activation of KillerRed in the AWB neuron resulted in its structural disruption after illumination, but had no effect on the structure of AWA (Figures 4A and 4B). Second, we examined cholinergic and GABAergic motor neurons. These neurons are synaptic partners; their cell bodies are located near the ventral nerve cord and their processes fasciculate together in the dorsal and ventral nerve cords (White et al., 1986). We found that KillerRed activation in the GABAergic neurons did not affect the morphology of the cholinergic neurons (Figures 4C and 4D). Furthermore, KillerRed activation in GABAergic neurons caused a GABAergic-specific functional defect (Figure 1A) rather than the coiled-paralysis defect caused by activation in cholinergic neurons (Figures 1F and 2). Similar specificity was observed when GABA neurons were imaged after KillerRed activation in the cholinergic neurons, that is, activation in cholinergic neurons did not affect the GABA neurons. Finally, we tested whether KillerRed activation in the PLM mechanosensory neuron had any effect on the morphology of the nearby PLN neuron. Both PLM and PLN neurons have their cell bodies in the lumbar ganglia, and their processes run adjacent to each other for the entire posterior half of an animal's body (White et al., 1986). Activation of KillerRed in PLM had no effect on the axon or cell body of PLN (Figures 4E–4G). Together, these results indicate that KillerRed-mediated functional disruption and cell damage is cell-autonomous and does not spread beyond the targeted cell (or cells).

Selective Illumination Results in Neuronal Cell Death

We next investigated the effect of selective illumination on different regions of the animal's body or on defined regions of

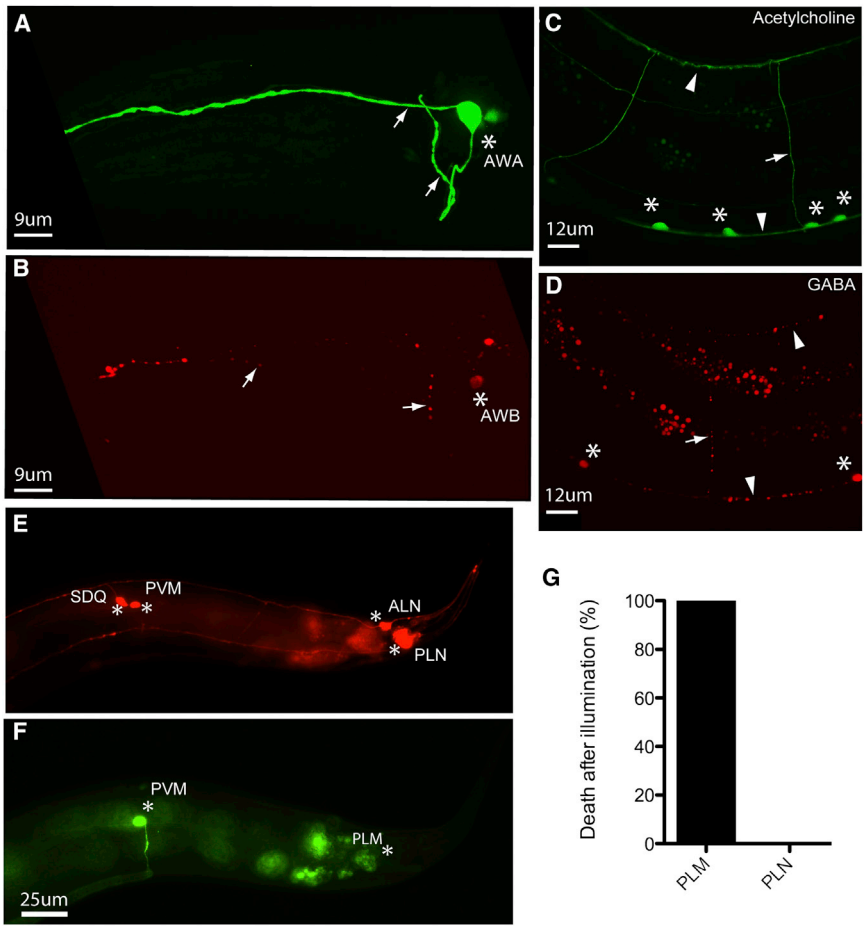

Figure 4. KillerRed Phototoxicity Does Not Spread to Neighboring Neurons

(A) AWA neuron intact after illumination (green, *Podr-10::GFP*).

(B) AWB degenerated neuron in the same animal as in (A) (red, *Pstr-1::myr-tdKillerRed*).

(C) Cholinergic neurons after illumination (green, *Punc-17::GFP*).

(D) Affected GABAergic neurons after illumination in the same animal as in (C) (red, *Punc-47::myr-tdKillerRed*).

(E) PLN neuron after illumination (red, *Plad-2::mCherry*).

(F) PLM neurons expressing KillerRed after illumination in the same animal as in (E) (green, *Pmec-4::GFP*). In all panels, asterisks mark cell bodies, arrows mark processes, and arrowheads mark dorsal (top) and ventral (bottom) nerve cords.

(G) Quantification of cell death in PLM and PLN neurons in animals expressing KillerRed in PLM only. Animals were scored for PLN death only if PLM had died; thus, PLM death is 100%. n = 25 animals in which both PLM and PLN were scored. In all panels, phenotypes were determined 24 hr after illumination.

See also Table S1.

individual neurons. For these experiments, we chose the mechanosensory neurons ALM and PLM and used a spatially restricted illumination scheme similar to that used previously for optogenetic stimulation and inhibition of neurons (Stirman et al., 2011). Specifically, we first imaged animals for GFP to locate the neurons expressing KillerRed without inducing cell damage. Then, using an LCD projector controlled by a LabVIEW program, we illuminated selected regions (such as the anterior half or posterior half of the animal's body, or the cell body or axon of a single neuron; Figure 5). Using high-magnification lenses with a small focal depth (e.g., 100×), we were able to confine illumination with precision and reproducibility. Targeting the anterior or posterior half of the animal induced cell death of specific neurons included in the respective illuminated regions (Figures 5A–5C). As was the case with the nontargeted illumination, AVM and PVM were resistant to KillerRed-induced damage. When activation was confined to a limited portion of a single neuron, we found that targeting only the cell body of the ALM mechanosensory neuron resulted in cell damage and death (Figures 5D and 5E). Similarly, when the illumination was directed selectively to the axon, we observed robust cell death (>40% of cases), with the remaining animals presenting axonal degeneration in regions beyond the irradiated sections. Thus, even though expression of KillerRed was not spatially limited, regional illumination was enough to produce KillerRed-mediated cell damage and death.

Mitochondrial Targeting Results in Organelle-Specific Effects

The experiments described above show that both membrane-targeted and cytoplasmic KillerRed can disrupt neuronal function and kill neurons. To test whether KillerRed function is dependent on subcellular localization, we targeted tandem dimeric KillerRed to mitochondria using the *tom-20* targeting sequence, which results in localization of KillerRed to the outer surface of the mitochondrion (Ichishita et al., 2008; Kanaji et al., 2000). We performed these experiments in body wall muscles because the mitochondria in these cells have a well-defined morphology, which enabled us to assess the effect of KillerRed on cell structure and function and on the mitochondria themselves. We found that KillerRed was efficiently targeted to mitochondria, and that mitochondria labeled with KillerRed (without activation) had normal morphology consisting of a reticulated network (Figure 6A). Further, animals that expressed mitochondria-targeted KillerRed (mt-tdKillerRed) in all of their body wall muscles displayed normal movement in the absence of light activation, demonstrating that muscle function was not disrupted by mt-tdKillerRed expression (data not shown). By contrast, when mt-tdKillerRed-expressing animals were exposed to green light, we observed an immediate and dramatic change in mitochondria morphology in muscle. mt-tdKillerRed activation disrupted the reticulated network of mitochondria and resulted in small, spherical mitochondria of various sizes (Figure 6B). Surprisingly, we did not observe behavioral deficits in these animals,

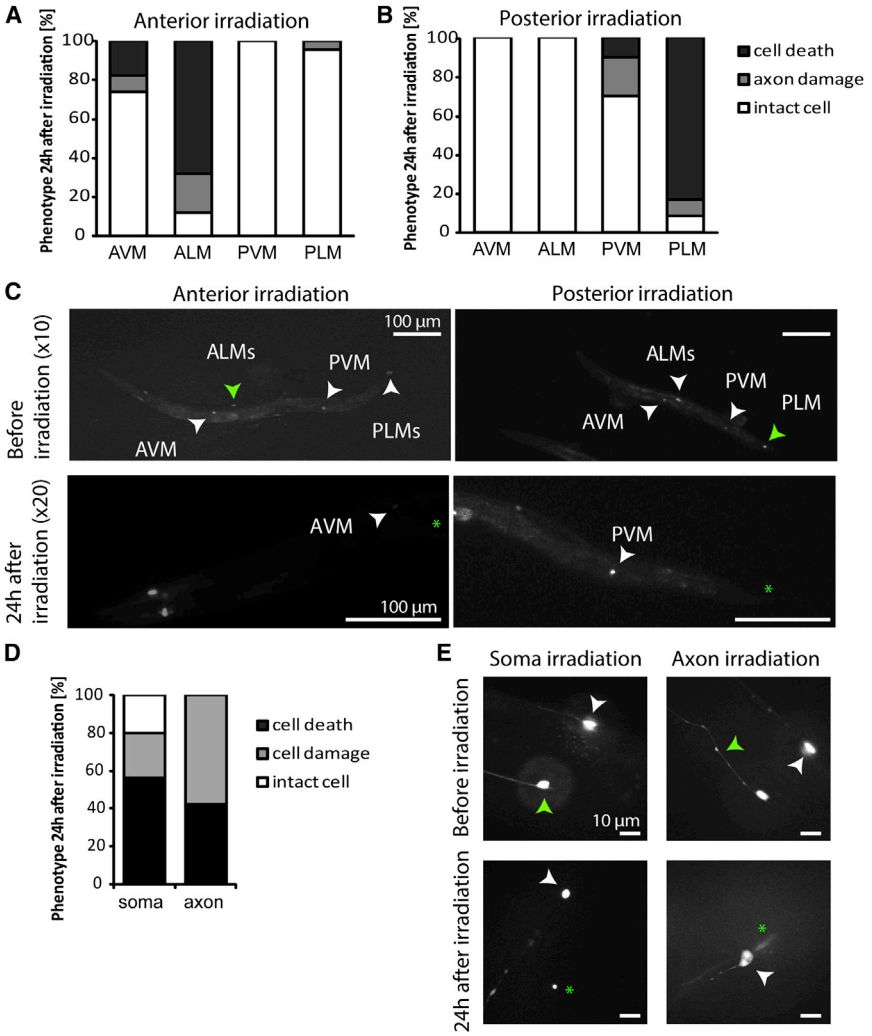

Figure 5. Selected Region Illumination Can Be Used in Combination with KillerRed to Induce Cell-Specific Killing

(A and C) Illumination of the anterior half body of the animal causes selective ablation of ALM neurons, whereas PLM neurons are intact. n = 25 animals.

(B and C) Illumination of the posterior half of the animal's body ablated PLM neurons, leaving intact ALMs. n = 24 animals.

(D and E) Selective illumination of either the soma or axon of ALM neurons can cause damage and neuronal ablation. n = 25 animals for soma and 19 animals for axon illumination. In all of the images, the green arrowhead points to the targeted neuron or axon before illumination, asterisks indicate the same cell 24 hr after illumination, and white arrowheads point to different neuronal cell bodies in the animal.

See also Table S1.

suggesting that activation of mt-tdKillerRed did not kill muscle cells (Figure 6G). By contrast, expression of plasma membrane-targeted KillerRed (myr-tdKillerRed) in the same muscle cells resulted in cell death and immediate behavioral deficits after activation (Figures 6E and 6F). Since mt-tdKillerRed did not kill muscles, we performed studies to test whether mitochondrial morphology could recover after KillerRed-mediated disruption. We found that by 48 hr after disruption, the mitochondria had recovered normal morphology (Figures 6C and 6D). Together, these results demonstrate that subcellular targeting of KillerRed enables the generation of local and specific cell-biological phenotypes.

Use of KillerRed with Other Optical Tools

A number of optical tools are currently being used in *C. elegans*, including the optogenetic tool channelrhodopsin (Nagel et al., 2005) and the reactive oxygen generator miniSOG (Qi et al., 2012). Because KillerRed is excited by green light, whereas these other tools are excited by blue light, we considered that it might be possible to address them separately in a single animal by using different illumination wavelengths. To determine the feasibility of this idea, we compared the requirements for activation of KillerRed, channelrhodopsin, and miniSOG in the cholinergic motor neurons. The activity of all three tools has been described in these cells (Figures 1F and 2; Liu et al., 2009; Qi et al., 2012; Zhang et al., 2007). First, we determined the feasibility of using KillerRed in combination with miniSOG. We irradiated animals expressing miniSOG in cholinergic motor neurons (CZ14527) using 0.57 mW/mm^2 of blue light for 30 min as previously described (Qi et al., 2012; Table S1). This treatment affected 100% of the animals: 42% were paralyzed and the remaining animals could move but were sluggish. Similarly, we irradiated animals expressing KillerRed in cholinergic neurons with the same intensity (0.57 mW/mm^2) and time of green light, and again observed 100% affected animals, with 76% paralysis and 24% sluggish movement (Figure 7A). Next, we swapped the illumination conditions, that is, we illuminated miniSOG animals with 0.57 mW/mm^2 of green light and KillerRed animals with 0.57 mW/mm^2 of blue. This treatment had little to no effect, although approximately 6% of the KillerRed animals did react to blue light illumination (Figure 7A). Finally, we asked whether higher-intensity activation could be used for miniSOG. We had previously observed that *C. elegans* can tolerate green light at 46 mW/mm^2 for 15 min with no adverse effects (other than KillerRed activation; Figure 1). However, exposing wild-type worms (n = 20) to blue light at 8 mW/mm^2 for 10 min resulted in 100% lethality, consistent with previous results (Edwards et al., 2008). Together, these data suggest that KillerRed and miniSOG can be separately addressed in vivo.

Next, we determined the feasibility of using KillerRed in conjunction with channelrhodopsin. Again, we focused on the

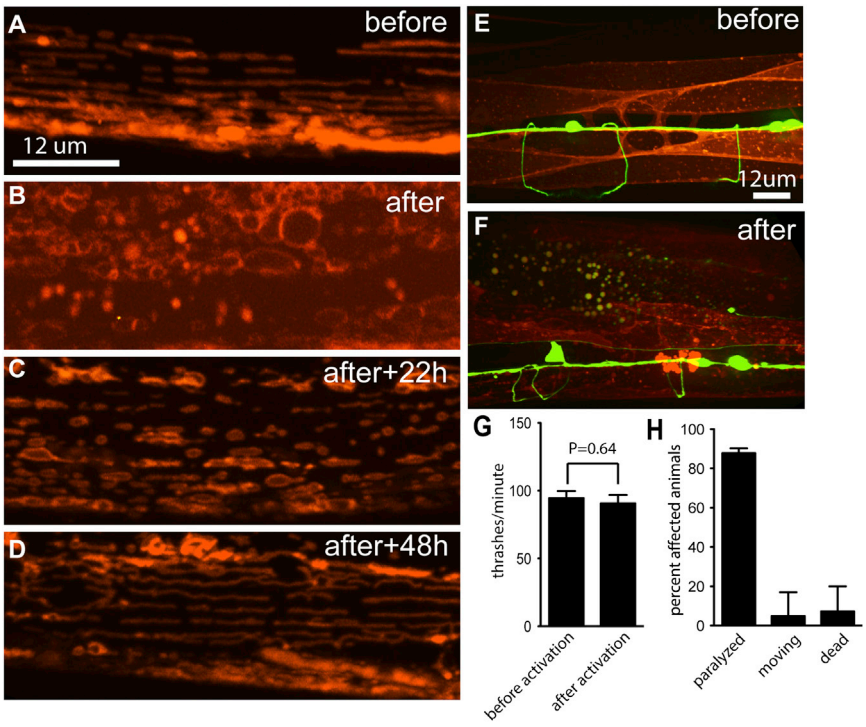

Figure 6. KillerRed Activation at Mitochondria Results in Organelle Damage but Cell Survival

(A–D) Mitochondria in body wall muscles express mt-tdKillerRed and were imaged before (A) or at various times after (B–D) illumination.

(E and F) Body wall muscles express plasma membrane KillerRed and were imaged before (E) and 16 hr after (F) illumination. GABA neurons express GFP.

(G) Average thrash rate in liquid of animals expressing mitochondria KillerRed in muscles before and after illumination, corresponding to (A) and (B). n = 9 for before illumination and 10 for after illumination; error bars indicate SEM.

(H) Phenotype distribution of animals expressing plasma membrane KillerRed in muscles after illumination, corresponding to (F). n = 41; error bars indicate 95% confidence intervals.

See also Table S1.

cholinergic motor neurons, which are a well-described site for channelrhodopsin activation (Liu et al., 2009; Zhang et al., 2007). We tested whether activation of channelrhodopsin could be performed independently of KillerRed activation. We activated channelrhodopsin in cholinergic motor neurons using 0.47 mW/mm^2 of blue light, which caused 100% of the animals to stop moving (n = 23). By contrast, 2.2 mW/mm^2 of green light had no effect on these animals (n = 22). As we previously determined that an even lower intensity of green light could be used to activate KillerRed, and a higher intensity of blue light could be used *without* activating KillerRed (Figure 7A), these experiments indicate that KillerRed can be used in multimodal experiments with channelrhodopsin. Finally, we confirmed these experiments in mechanosensory neurons. As in the cholinergic neurons, we found that prolonged illumination of KillerRed strains at the appropriate wavelength and intensity to activate channelrhodopsin had very little effect, although axon damage was observed in a small percentage of animals (Figures 7B and 7C). These data confirm that KillerRed can be used in conjunction with channelrhodopsin in *C. elegans*, as well as in conjunction with other fluorescent tools that are excited by blue or cyan light.

DISCUSSION

KillerRed is a new tool in the *C. elegans* optogenetic toolkit that can kill and inactivate cells in populations of animals with extremely high temporal and spatial control. The effect of KillerRed is immediate and cell-autonomous, with no spreading of killing, or even damage, to surrounding cells or tissues. This critical property makes KillerRed a powerful biological tool that can be applied in a wide variety of cell-perturbation studies in vivo, at scales ranging from single to multiple cells in both single animals and populations. For example, the rapidity and efficacy of this genetically encoded cell-ablation reagent will now allow investigators to examine the acute effects of disrupting specific neurons during behavioral performance. KillerRed can also be used for longer behavioral studies, since ablated neurons never recover function. For example, our data indicate that GABA neurons have an essential function in the locomotion of L1 larvae. Similarly, our data indicate that ablation of acetylcholine neurons in L4 stage animals results in relatively rapid lethality (within 24 hr of ablation), suggesting that *C. elegans* has an acute requirement for cholinergic neurotransmission for viability. One potential concern for such behavioral studies is the fact that because KillerRed damages and kills neurons, rather than merely silencing them, it is possible that secondary effects on the remaining cells in the network might complicate analysis. However, our data demonstrate that, at least for the neurons assessed here, the effects of ablation are restricted to the cells that express KillerRed.

Further, because KillerRed is excited by green light, it can be used in combination with other optogenetic tools that are excited by blue light, such as GFP, GCaMP, channelrhodopsin, and miniSOG. The green light activation of KillerRed may have some additional practical advantages in *C. elegans*, as worms tolerate high levels of green light, but actively avoid—and can be killed by—equivalent amounts of blue light (Edwards et al., 2008). The selective-illumination method we describe here may also have additional applications, such as ablating a neuron from a distance by targeting a region of its axon (this is particularly important when using KillerRed expressed in cells whose cell bodies are in very close proximity and therefore are more difficult to target individually), and investigating ROS effects in axonal sections.

Our results also indicate that subcellular localization of KillerRed can be exploited to study specific cell-biological

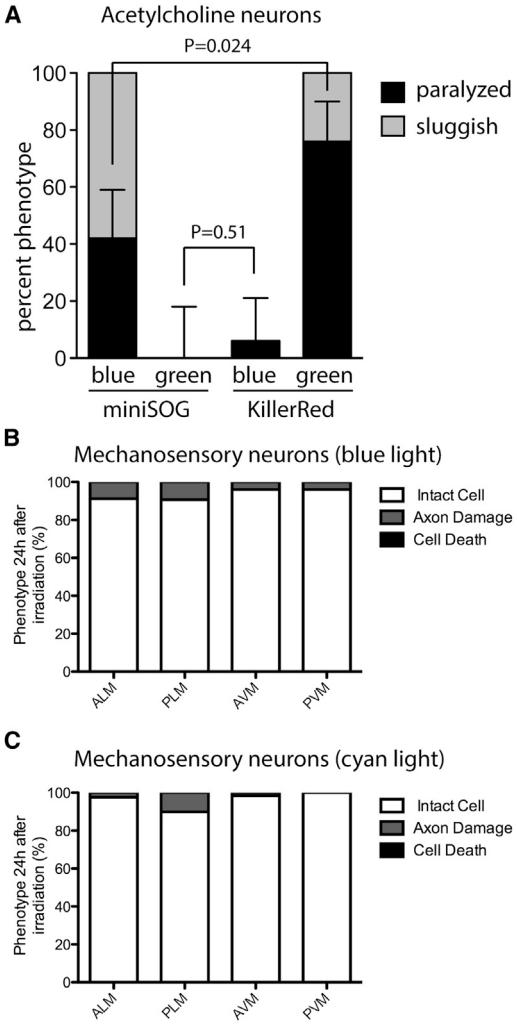

Figure 7. KillerRed Can Be Used in Multimodal Optical Experiments

(A) Comparison of the effects of KillerRed and miniSOG in acetylcholine neurons illuminated with either blue or green light. n = 33 for miniSOG/blue, n = 21 for miniSOG/green, n = 32 for KillerRed/blue, and n = 21 for KillerRed/green. Error bars show 95% confidence interval for the paralyzed phenotype. Phenotypes were determined 10 min after illumination.

(B and C) Effect of KillerRed in mechanosensory neurons illuminated with either blue (b) or cyan (c) light. n = 102 for blue light and n = 64 for cyan light. Phenotypes were determined 24 hr after illumination.

See also Table S1.

functions. Targeting and activating KillerRed at the plasma membrane is sufficient to inactivate and kill cells. This rapid and lethal effect could be due to the susceptibility of membrane lipids to oxidation. For example, unsaturated lipids are highly susceptible to oxidative stress, resulting in the generation of toxic compounds such as hydroxynonenal and acrolein (Catalá, 2010; Fatokun et al., 2008). In addition to causing loss of membrane fluidity and destruction of the plasma membrane barrier, these toxic compounds react with membrane proteins, resulting in inactivation of critical proteins such as the neuronal glucose transporter, the glutamate transporter, and Na^+/K^+ ATPases (Barnham et al., 2004; Keller et al., 1997; Mark et al., 1995; Smith et al., 2009). In contrast, targeting and activating KillerRed at mitochondria results in the specific disruption (and eventual recovery) of organelle morphology, without killing cells. A potential explanation for the local effect of KillerRed on mitochondria is that ROS are quenched rapidly and thus the effective diffusion rate is very low. Alternatively, it is possible that the TOM20 tag affects KillerRed function, allowing for mitochondrial damage but preventing cell killing. Interestingly, another optogenetic reactive oxygen generator, miniSOG, requires mitochondrial targeting to kill neurons (Qi et al., 2012). miniSOG generates mainly singlet oxygen, whereas KillerRed generates mainly superoxide (Pletnev et al., 2009; Shu et al., 2011; this work). These data suggest that different ROS may affect mitochondria and cell function in different ways. KillerRed thus enables the dissection of local effects of ROS.

ROS are toxic cellular molecules that need to be kept in check for a neuron to function over a long period of time, and ROS accumulation correlates with a variety of neurodegenerative diseases (DiMauro and Schon, 2008; Uttara et al., 2009). Therefore, defining the nature of the cytotoxicity of KillerRed, a generator of ROS, offers a significant opportunity to genetically investigate the mechanisms that regulate cellular responses to ROS. Our findings show that selective neurons, such as AVM, PVM, and AWB, are resistant to damage caused by KillerRed activation and ROS. KillerRed expression is weaker in PVM than in other neurons, so the reduced killing effect could be due to the presence of fewer molecules in the cell. However, AVM and AWB express KillerRed at levels comparable to those observed in other neurons, suggesting that they might have a higher intrinsic capacity to buffer ROS. One such mechanism could be a higher expression of molecules, such as SOD-1, that are able to catabolize ROS into nontoxic elements. Our data demonstrating that a mutation in SOD-1 is able to increase the cytotoxic effect of KillerRed activation in AWB provide support for this idea, although additional mechanisms might also be in place. We expect that the application of KillerRed shown here will provide greater flexibility and control for genetic studies of both neuronal function and ROS-induced neuronal damage in vivo.

EXPERIMENTAL PROCEDURES

Strains and Molecular Biology

Nematodes were cultured using standard methods. All experiments were performed at 22°C except when otherwise noted. A *C. elegans* version of the KillerRed coding sequence was synthesized (GenScript) using worm-optimized codons and synthetic introns (Fire et al., 1990; Stenico et al., 1994). Flanking regions for Multisite Gateway (Invitrogen) were included and the KillerRed construct was placed in pDONR221. tdKillerRed was generated from this monomeric construct using the same linker sequences as tdTomato (Serebrovskaya et al., 2009; Shaner et al., 2004). tdKillerRed was targeted to the plasma membrane through the addition of a myristoylation tag to generate myr-tdKillerRed (Gitai et al., 2003). Promoters were cloned into the [4-1] slot of Multisite Gateway. Final expression constructs were generated with LR clonase into the destination vector pCFJ150 (Frøkjaer-Jensen et al., 2010). For experiments with the mechanosensory neurons, we used the following transgenes and mutations: *zdIs5(Pmec-4::GFP)*, *vdEx405[Pmec-4::KillerRed* (20 ng/μl) + *odr-1::DsRED* (30 ng/μl)], LGIV *ced-3(n717)*, and *vdEx167[Plad-2::mCherry* (25 ng/μl) + *Podr-1::dsRED* (30 ng/μl)]; Neumann et al., 2011). Standard molecular-biology methods were used. The *Pmec-4::KR* construct was generated by cloning a KillerRed cDNA (Evrogen) into a pSM vector

(a derivative of pPD49.26 [Fire et al., 1990], a kind gift from Steve McCarroll and Cori Bargmann) containing *Pmec-4*. KillerRed was amplified with primers containing BamHI restrictions sites and inserted into pSM *Pmec-4* digested with the same enzyme.

DNA constructs were injected into the germline using standard methods (Mello et al., 1991). Expression of KillerRed in the correct cells was verified by fluorescence microscopy.

KillerRed Activation and Imaging

Light from a 200 W mercury bulb (PhotoFluor II; 89 North) was filtered with a 562/20 nm filter. The resulting green light was trained into a 5 mm liquid-light guide. The output from the liquid-light guide was directed through a collimating lens (LA1951-A; Thorlabs) and a focusing lens (LA1027-A). Light intensity was measured with a power meter (PM100A; Thorlabs). Illuminations were done in upside-down PCR tube caps in 30 μl of M9 medium on ice to minimize sample heating. L4 stage transgenic worms were used in all experiments. The animals were allowed to crawl on unseeded plates prior to the experiment to remove excess bacteria. Different neuronal cell types required different illumination protocols to result in optimal killing. Illumination times, light intensities, and transgenic lines carrying myr-tdKillerRed are shown in Table S1. An UltraVIEW VoX (PerkinElmer) spinning disc mounted on a Nikon Ti-E Eclipse inverted microscope and a 60× CFI Plan Apo, NA 1.0 oil objective were used to capture z stacks of nonilluminated and illuminated neurons. Cellular damage in illuminated neurons was documented 18–24 hr after illumination.

Illumination of mechanosensory neurons was performed on animals immobilized on NGM agar plates with tetramisole hydrochloride (0.03%), using a Leica MZ10F fluorescence dissecting microscope with an EtDsRed filter (green light 530–560 nm) and 80× magnification (intensity 3.8 mW/mm^2). Twenty-four hours after irradiation, the animals were mounted on 4% agar pads and visualized by epifluorescence using a Zeiss Axioimager Z1 and a Zeiss Axioimager A1 microscope. A CoolSNAP HQ^2 camera (Photometrics) was used for imaging. Metamorph software was used to analyze the collected images.

Selective illumination was performed using the LCD projector system as previously described (Stirman et al., 2011). GFP fluorescence was used to image the cells and define the location of the soma and axon. A green filter (543–593 nm) was used to activate KR in regions of interest selected after imaging. Typical power densities were 2–3 mW/mm^2. In all experiments performed using this system, the illumination time was 1 hr. The length of the axonal processes that were selectively illuminated was 80 μm in all cases. Extensive degeneration was defined as damage that extended beyond 10% of the illuminated length along the axon.

Acute KillerRed activation using freely swimming worms was performed on a modified version of the COLBERT system (Leifer et al., 2011). Briefly, a freely moving L1 larva was imaged with a 20× microscope objective on an inverted Nikon microscope (TE2000). The fluorescence video was taken with a CoolSNAP CCD camera (Photometrics). A digital micromirror device was used to reflect green laser light to illuminate targeted regions of the worm, inducing KillerRed activation in GABAergic motor neurons.

Activation of miniSOG was performed using the same Photofluor II system employed for KillerRed, but with a filter at the appropriate wavelength (Table S1).

Statistics

Statistical comparisons were made using the two-tailed Fisher's exact test (http://www.graphpad.com/quickcalcs/contingency1/), and 95% confidence intervals were calculated using http://www.graphpad.com/quickcalcs/confInterval1/.

SUPPLEMENTAL INFORMATION

Supplemental Information includes one table and two movies and can be found with this article online at http://dx.doi.org/10.1016/j.celrep.2013.09.023.

ACKNOWLEDGMENTS

We thank Brent Neumann, Rosina Giordano-Santini, and Rowan Tweedale for reading the manuscript, and Luke Hammond for technical assistance.

Work in the Hammarlund lab is supported by the Ellison Medical Foundation and NIH grant R01NS066082 to M.H. Work in the Hilliard lab is supported by NHMRC Project Grants 569500 and 631634, and an ARC Future Fellowship to M.A.H. S.C. was supported by an Australian Postgraduate Award. Work in the Lu lab is supported by grants from the NSF, NIH (R01GM088333, R21EB012803, and R01AG035317), Sloan Foundation, and Human Frontiers Science Program to H.L. Work in the Samuel lab is supported by an NIH Pioneer Award, the NSF, and the Harvard-MIT Joint Research Grants Program. D.C.W. was supported by American Cancer Society grant PF-07-037-01-CSM.

Received: March 26, 2013
Revised: August 1, 2013
Accepted: September 13, 2013
Published: October 24, 2013

REFERENCES

Alfonso, A., Grundahl, K., Duerr, J.S., Han, H.-P., and Rand, J.B. (1993). The Caenorhabditis elegans unc-17 gene: a putative vesicular acetylcholine transporter. Science *261*, 617–619.

Avery, L., and Horvitz, H.R. (1987). A cell that dies during wild-type C. elegans development can function as a neuron in a ced-3 mutant. Cell *51*, 1071–1078.

Avery, L., and Horvitz, H.R. (1989). Pharyngeal pumping continues after laser killing of the pharyngeal nervous system of C. elegans. Neuron *3*, 473–485.

Barnham, K.J., Masters, C.L., and Bush, A.I. (2004). Neurodegenerative diseases and oxidative stress. Nat. Rev. Drug Discov. *3*, 205–214.

Bulina, M.E., Chudakov, D.M., Britanova, O.V., Yanushevich, Y.G., Staroverov, D.B., Chepurnykh, T.V., Merzlyak, E.M., Shkrob, M.A., Lukyanov, S., and Lukyanov, K.A. (2006). A genetically encoded photosensitizer. Nat. Biotechnol. *24*, 95–99.

Campbell, R.E., Tour, O., Palmer, A.E., Steinbach, P.A., Baird, G.S., Zacharias, D.A., and Tsien, R.Y. (2002). A monomeric red fluorescent protein. Proc. Natl. Acad. Sci. USA *99*, 7877–7882.

Carpentier, P., Violot, S., Blanchoin, L., and Bourgeois, D. (2009). Structural basis for the phototoxicity of the fluorescent protein KillerRed. FEBS Lett. *583*, 2839–2842.

Catalá, A. (2010). A synopsis of the process of lipid peroxidation since the discovery of the essential fatty acids. Biochem. Biophys. Res. Commun. *399*, 318–323.

Chow, B.Y., Han, X., Dobry, A.S., Qian, X., Chuong, A.S., Li, M., Henninger, M.A., Belfort, G.M., Lin, Y., Monahan, P.E., and Boyden, E.S. (2010). High-performance genetically targetable optical neural silencing by light-driven proton pumps. Nature *463*, 98–102.

DiMauro, S., and Schon, E.A. (2008). Mitochondrial disorders in the nervous system. Annu. Rev. Neurosci. *31*, 91–123.

Edwards, S.L., Charlie, N.K., Milfort, M.C., Brown, B.S., Gravlin, C.N., Knecht, J.E., and Miller, K.G. (2008). A novel molecular solution for ultraviolet light detection in Caenorhabditis elegans. PLoS Biol. *6*, e198.

Ellis, H.M., and Horvitz, H.R. (1986). Genetic control of programmed cell death in the nematode C. elegans. Cell *44*, 817–829.

Fang-Yen, C., Gabel, C.V., Samuel, A.D.T., Bargmann, C.I., and Avery, L. (2012). Laser microsurgery in Caenorhabditis elegans. Methods Cell Biol. *107*, 177–206.

Fatokun, A.A., Stone, T.W., and Smith, R.A. (2008). Oxidative stress in neurodegeneration and available means of protection. Front. Biosci. *13*, 3288–3311.

Fire, A., Harrison, S.W., and Dixon, D. (1990). A modular set of lacZ fusion vectors for studying gene expression in Caenorhabditis elegans. Gene *93*, 189–198.

Frøkjaer-Jensen, C., Davis, M.W., Hollopeter, G., Taylor, J., Harris, T.W., Nix, P., Lofgren, R., Prestgard-Duke, M., Bastiani, M., Moerman, D.G., and Jorgensen, E.M. (2010). Targeted gene deletions in C. elegans using transposon excision. Nat. Methods *7*, 451–453.

Gitai, Z., Yu, T.W., Lundquist, E.A., Tessier-Lavigne, M., and Bargmann, C.I. (2003). The netrin receptor UNC-40/DCC stimulates axon attraction and outgrowth through enabled and, in parallel, Rac and UNC-115/AbLIM. Neuron *37*, 53–65.

Hall, D.H., Gu, G., García-Añoveros, J., Gong, L., Chalfie, M., and Driscoll, M. (1997). Neuropathology of degenerative cell death in Caenorhabditis elegans. J. Neurosci. *17*, 1033–1045.

Ichishita, R., Tanaka, K., Sugiura, Y., Sayano, T., Mihara, K., and Oka, T. (2008). An RNAi screen for mitochondrial proteins required to maintain the morphology of the organelle in Caenorhabditis elegans. J. Biochem. *143*, 449–454.

Kanaji, S., Iwahashi, J., Kida, Y., Sakaguchi, M., and Mihara, K. (2000). Characterization of the signal that directs Tom20 to the mitochondrial outer membrane. J. Cell Biol. *151*, 277–288.

Keller, J.N., Pang, Z., Geddes, J.W., Begley, J.G., Germeyer, A., Waeg, G., and Mattson, M.P. (1997). Impairment of glucose and glutamate transport and induction of mitochondrial oxidative stress and dysfunction in synaptosomes by amyloid β-peptide: role of the lipid peroxidation product 4-hydroxynonenal. J. Neurochem. *69*, 273–284.

Landis, G.N., and Tower, J. (2005). Superoxide dismutase evolution and life span regulation. Mech. Ageing Dev. *126*, 365–379.

Leifer, A.M., Fang-Yen, C., Gershow, M., Alkema, M.J., and Samuel, A.D.T. (2011). Optogenetic manipulation of neural activity in freely moving Caenorhabditis elegans. Nat. Methods *8*, 147–152.

Liu, Q., Hollopeter, G., and Jorgensen, E.M. (2009). Graded synaptic transmission at the Caenorhabditis elegans neuromuscular junction. Proc. Natl. Acad. Sci. USA *106*, 10823–10828.

Mark, R.J., Hensley, K., Butterfield, D.A., and Mattson, M.P. (1995). Amyloid beta-peptide impairs ion-motive ATPase activities: evidence for a role in loss of neuronal Ca2+ homeostasis and cell death. J. Neurosci. *15*, 6239–6249.

McIntire, S.L., Jorgensen, E., Kaplan, J., and Horvitz, H.R. (1993). The GABAergic nervous system of Caenorhabditis elegans. Nature *364*, 337–341.

McIntire, S.L., Reimer, R.J., Schuske, K., Edwards, R.H., and Jorgensen, E.M. (1997). Identification and characterization of the vesicular GABA transporter. Nature *389*, 870–876.

Mello, C.C., Kramer, J.M., Stinchcomb, D., and Ambros, V. (1991). Efficient gene transfer in C. elegans: extrachromosomal maintenance and integration of transforming sequences. EMBO J. *10*, 3959–3970.

Nagel, G., Brauner, M., Liewald, J.F., Adeishvili, N., Bamberg, E., and Gottschalk, A. (2005). Light activation of channelrhodopsin-2 in excitable cells of Caenorhabditis elegans triggers rapid behavioral responses. Curr. Biol. *15*, 2279–2284.

Neumann, B., Nguyen, K.C.Q., Hall, D.H., Ben-Yakar, A., and Hilliard, M.A. (2011). Axonal regeneration proceeds through specific axonal fusion in transected C. elegans neurons. Dev. Dyn. *240*, 1365–1372.

Okazaki, A., Sudo, Y., and Takagi, S. (2012). Optical silencing of C. elegans cells with arch proton pump. PLoS ONE *7*, e35370.

Pletnev, S., Gurskaya, N.G., Pletneva, N.V., Lukyanov, K.A., Chudakov, D.M., Martynov, V.I., Popov, V.O., Kovalchuk, M.V., Wlodawer, A., Dauter, Z., and Pletnev, V. (2009). Structural basis for phototoxicity of the genetically encoded photosensitizer KillerRed. J. Biol. Chem. *284*, 32028–32039.

Qi, Y.B., Garren, E.J., Shu, X., Tsien, R.Y., and Jin, Y. (2012). Photo-inducible cell ablation in Caenorhabditis elegans using the genetically encoded singlet oxygen generating protein miniSOG. Proc. Natl. Acad. Sci. USA *109*, 7499–7504.

Rand, J.B. (1989). Genetic analysis of the cha-1-unc-17 gene complex in Caenorhabditis. Genetics *122*, 73–80.

Roy, A., Carpentier, P., Bourgeois, D., and Field, M. (2010). Diffusion pathways of oxygen species in the phototoxic fluorescent protein KillerRed. Photochem. Photobiol. Sci. *9*, 1342–1350.

Serebrovskaya, E.O., Edelweiss, E.F., Stremovskiy, O.A., Lukyanov, K.A., Chudakov, D.M., and Deyev, S.M. (2009). Targeting cancer cells by using an antireceptor antibody-photosensitizer fusion protein. Proc. Natl. Acad. Sci. USA *106*, 9221–9225.

Shaner, N.C., Campbell, R.E., Steinbach, P.A., Giepmans, B.N.G., Palmer, A.E., and Tsien, R.Y. (2004). Improved monomeric red, orange and yellow fluorescent proteins derived from Discosoma sp. red fluorescent protein. Nat. Biotechnol. *22*, 1567–1572.

Shu, X., Lev-Ram, V., Deerinck, T.J., Qi, Y., Ramko, E.B., Davidson, M.W., Jin, Y., Ellisman, M.H., and Tsien, R.Y. (2011). A genetically encoded tag for correlated light and electron microscopy of intact cells, tissues, and organisms. PLoS Biol. *9*, e1001041.

Smith, A.J., Smith, R.A., and Stone, T.W. (2009). 5-Hydroxyanthranilic acid, a tryptophan metabolite, generates oxidative stress and neuronal death via p38 activation in cultured cerebellar granule neurones. Neurotox. Res. *15*, 303–310.

Stenico, M., Lloyd, A.T., and Sharp, P.M. (1994). Codon usage in Caenorhabditis elegans: delineation of translational selection and mutational biases. Nucleic Acids Res. *22*, 2437–2446.

Stirman, J.N., Crane, M.M., Husson, S.J., Wabnig, S., Schultheis, C., Gottschalk, A., and Lu, H. (2011). Real-time multimodal optical control of neurons and muscles in freely behaving Caenorhabditis elegans. Nat. Methods *8*, 153–158.

Teh, C., Chudakov, D.M., Poon, K.-L., Mamedov, I.Z., Sek, J.-Y., Shidlovsky, K., Lukyanov, S., and Korzh, V. (2010). Optogenetic in vivo cell manipulation in KillerRed-expressing zebrafish transgenics. BMC Dev. Biol. *10*, 110.

Uttara, B., Singh, A.V., Zamboni, P., and Mahajan, R.T. (2009). Oxidative stress and neurodegenerative diseases: a review of upstream and downstream antioxidant therapeutic options. Curr. Neuropharmacol. *7*, 65–74.

White, J.G., Southgate, E., Thomson, J.N., and Brenner, S. (1986). The structure of the nervous system of the nematode Caenorhabditis elegans. Philos. Trans. R. Soc. Lond. B Biol. Sci. *314*, 1–340.

Zhang, F., Wang, L.-P., Brauner, M., Liewald, J.F., Kay, K., Watzke, N., Wood, P.G., Bamberg, E., Nagel, G., Gottschalk, A., and Deisseroth, K. (2007). Multimodal fast optical interrogation of neural circuitry. Nature *446*, 633–639.